Journal of Applied Polymer Science

Synthesis of Hybrid ZnO/CNTs Nanoparticles and Their Reinforcement in Nylon-6 Polymer Fibers

Vijaya K. Rangari,[1] Ghouse M. Mohammad,[1] Boyoglu, Seyhan,[2] Shaik Jeelani[1]
[1]Department of Materials Science and Engineering, Tuskegee University, Tuskegee, Alabama 36088
[2]Center for NanoBiotechnology Research, Alabama State University, Montgomery, Alabama
Correspondence to: V. Rangari (E-mail: rangariv@mytu.tuskegee.edu)

ABSTRACT: In this investigation, *in situ* synthesis of zinc oxide nanoparticles in the presence of multiwalled carbon nanotubes (CNTs) have been carried out using a sonochemical technique. Zinc(II)acetate was used as a source of ZnO in the presence of ethylene glycol (EG) to obtain zinc oxide (ZnO) nanoparticles. The synthesized hybrid ZnO/CNTs nanoparticles were used as reinforcements to enhance the mechanical, thermal and UV absorbing properties of Nylon-6 composite fibers. The polymer nanocomposites (PNC) were fabricated by dry mixing Nylon-6 polymer powder with the ZnO/CNTs hybrid nanoparticles as the first step, then followed by the drying and melt extrusion process of fiber materials in a single-screw extruder. The extruded fibers were stretched and stabilized using a godet set-up and wound on a Wayne filament winder machine. The hybrid ZnO/CNTs infused Nylon-6 composite fibers were compared with commercial ZnO, CNTs infused Nylon-6 composite fibers and neat Nylon-6 fibers for their structural and thermal properties. The morphological characteristics of ZnO/CNTs nanoparticles were carried out using X-ray diffraction and transmission electron microscopy (TEM) techniques. The Nylon-6 PNC fibers which were of ~80 μ size were tested mechanically. The tensile tests revealed that failure stress of the 1% infused ZnO/CNTs Nylon-6 PNC fibers is about 73% higher than the neat extruded Nylon-6 fiber and the improvement in the tensile modulus is 377.4%. The DSC results show an increase in the glass transition temperature and crystallization for ZnO/CNTs infused Nylon-6 PNC fibers. © 2012 Wiley Periodicals, Inc. J. Appl. Polym. Sci. 129: 121–129, 2013

KEYWORDS: mechanical properties; thermoplastics; X-ray; synthesis; processing; composites

Received 9 July 2012; accepted 12 October 2012; published online 3 November 2012
DOI: 10.1002/app.38714

INTRODUCTION

Nanocomposites are a distinct form of composite materials, which involve imbedding nano or molecular domain sized particles into organic polymer, metal, or ceramic matrix materials. In all cases, it is perceived that the intimate inclusion of these nanoparticles in the matrices can drastically change the properties of these materials. In general, these NPs can be categorized into carbon-based materials such as fullerenes and CNTs and inorganic nanoparticles, including the ones based on metal oxides (zinc oxide, iron oxide, titanium dioxide, and cerium oxide), metals (gold, silver, and iron), and quantum dots (cadmium sulfide and cadmium selenide). In addition, these nanomaterials also present different interesting morphologies such as spheres, tubes, rods, and prisms[1]. The nanoparticles can serve as matrix reinforcement as well as change the electrical and thermal behavior of these base materials. The reason for this is that with such small inclusions, a large amount of interfacial phase material is created in the bulk of these nanocomposites. Zinc oxide is an n-type semiconductor with many attractive features. As a promising semiconductor material with a wide bandgap of 3.37 eV and a large excitation binding energy (60 meV) at room temperature,[2] ZnO has received widespread attention as optoelectronic materials because of its excellent performance in electronics, optics, and photonics systems.[3] It also has a potential application in photocatalytic degradation of organic pollutants under UV–vis light.[4] For photocatalytic reactions, ZnO nanoparticles have several advantages such as high optical activity and stability, high sensitivity for UV–vis light, and low fabrication cost.[5,6] Starowicz et al. showed that this band-gap semiconductor has numerous potential applications, particularly in the form of thin films, nanowires, nanorods, or nanoparticles and can be introduced to optoelectronic and electronic devices.[7] They also can be used in the production of chemical sensors and solar cells.[8] ZnO nanowires have attracted much attention for use as transparent electrodes in laser diodes or light-emitting diodes, chemical sensors, heat reflectors, surface acoustic wave devices, low-loss wave guides, and so on.[9] One of the most remarkable commercial applications of 20–100 nm ZnO nanoparticles is that their use in the production of sunscreens and cosmetics, because of their property of blocking

broad UV-A and UV-B rays.[10] This is a potentially important diffuse source of NP contamination, because of wash off from individuals into the environment. The ZnO nanoparticles are believed to be nontoxic, safe and biocompatible nanomaterial,[11] and compatible with skin, making it a suitable additive for textiles and surfaces that come in contact with humans. Although some reports have indicated toxicological activity of ZnO nanoparticles (e.g., in algae)[12] in the literature. It has been shown that they cause membrane damage in *E. coli*, possibly due to oxidative stress mechanisms.[13] Several methods have been explored for the synthesis of ZnO nanoparticles. Singh and Gopal[14] have reported the synthesis of ZnO nanoparticles by pulsed laser ablation of zinc target in aqueous media with simultaneous flow of pure oxygen gas. He et al.[15,16] reported a simple method for fabrication of uniform and ordered ZnO nanowires on Si substrates. In contrast, carbon nanotubes (CNTs) have attracted considerable attention since their discovery[17] because of their special structure, extraordinary mechanical and unique electronic properties, and unique applications. The CNTs exhibit a record of high Young's modulus and good elasticity,[18,19] and they are expected to be effective reinforcements in composite materials. Many studies on CNTs/polymer composites have revealed that good dispersion[20–23] and strong interfacial bonding[24] between CNTs and the polymer matrix result in strong reinforcement of the polymers. Rangari et al. aligned the pristine carbon nanotubes (P-CNTs) and fluorinated carbon nanotubes (F-CNTs) in Nylon-6 polymer composite fibers (PCFs) using single-screw extrusion method and shown a significant mechanical and thermal property improvements.[25] As two important building blocks in nanotechnology, ZnO nanoparticles and CNTs, have been assembled as hybrid structures[26–29] for various application. Park and coworkers[30] reported the coating of ZnO nanorods on CNTs by chemical vapor deposition in a tube furnace. Very recently, Chrissanthopoulos et al.[31] prepared ZnO/CNTs heterostructures by means of a thermal evaporation method. Rangari et al. reported on the general sonochemical synthesis of metal oxides from metal acetates using water-*N*,*N* dimethylformamide (DMF) as solvents.[32] Sonochemical processing has been proven as a useful technique for generating novel materials with unusual properties. The application of nanoparticles in textile materials has been the object of several studies aimed at producing finished fabrics with different performances. Alessio Becheri et al. reported the synthesis and characterization of nanosized ZnO particles and their application on cotton and wool fabrics for UV shielding.[33] Fiber-reinforced polymer composites are used in many structural applications because of their improvement in strength and toughness over the neat polymer. Polymers such as Nylon-6, polypropylene, and LDPE when mixed with appropriate percentage of nanoparticles as filler materials show significant improvements.[34] Many studies have been made on the structural, chemical, and thermal characterization of nylon.[35] Nylons are also employed to reinforce concrete for building construction applications. Among thermoplastic polymers, Nylon polymers are widely used materials due to their significant advantages such as low material cost, low density (~12.5% the weight of bronze, 14.3% the weight of cast iron, and 50% the weight of aluminum) wide range of available properties, corrosion resistance, compound customization, insulation qualities, and good load bearing capacity.[36,37] To study the synergistic effect of hybrid nanoparticles and Nylon-6 polymer, we have carried out the *in situ* synthesis of ZnO nanoparticles coated CNTs using sonochemical technique and infused these hybrid NPs in the Nylon-6 fiber using single screw extruder and tested for their thermal, mechanical, and UV absorbing properties.

EXPERIMENTAL

Materials

The CNTs (with outside diameter 10–20 nm, length 10–30 μm) were supplied by Nanostructure and Amorphous Materials (Houston, Texas, USA). Zinc (II) acetate, ethylene glycol, and Cetyltrimethyl ammonium bromide (CTAB) reagent grade with purity Œ99% was purchased from Sigma Aldrich. Commercial grade UBE nylon P1011F (Nylon-6, commercial name- Polyamide 6) was procured from UBE America (USA). The density of Nylon-6 is 1.09–1.19 g/cm^3, while the melting point is around 225°C. The mechanical property data as provided by the supplier are: tensile strength, 70–80 MPa; tensile elongation at break, 100%; and tensile modulus, 1–3 GPa.

In Situ Synthesis of Hybrid Zinc Oxide Nanoparticles Coated CNTs

In situ synthesis of ZnO coated CNTs (ZnO/CNTs) nanoparticles were carried out using dimethylformamide (DMF), EG, and 10% water-DMF, 10% water-EG as solvents. For example, in a typical synthesis of ZnO coated CNTs (ZnO/CNTs) nanoparticles was carried out using an ultrasonic irradiation of 90% ethylene glycol (EG) and 10% double distilled water solutions of Zinc (II) acetate precursor salt. As the CNTs have the tendency to agglomerate and form bundles together, a 10 mg of CNTs were magnetically stirred in a 150 mL of 90% EG and 10% water mixture for 15 min in a glass flask to uniformly disperse the CNTs in the solution. Then 250 mg of cetyltrimethyl ammonium bromide (CTAB) is used as a surfactant in the solution. A total of 500 mg of zinc (II) acetate was then added to the solution and was magnetically stirred for another 10 min using the magnetic stirrer for uniform dispersion of CNTs, Zinc (II) acetate salt, and CTAB in the solution before the ultrasonic irradiation reaction. Sonics Vibra Cell Ultrasonic processor (Ti-horn, 20 kHz, 100 W/cm^2) was used as a ultrasonic irradiation source. Ultrasonic irradiation utilizes high energy sonic waves to produce chemical reactions. The chemical effects of ultrasound arise from acoustic cavitations involving the formation, growth, and collapse of bubbles in liquid, which generates localized hot spots of a temperature ~5000 K, pressure of about 20 Mpa, and very high cooling rates of about 10^7 K/s.[38,39] The magnetically stirred solution of metal salt, surfactant, solvent, and CNTs is then sonochemically reacted for 2 h at 55% of amplitude with an external thermostat cooling at room temperature.

The purity of the product depends on the type of solvent used, the solubility of the salt in the solvent and the reaction parameters. The amount of CNTs used for the reaction depends on the yield of the nanoparticles from the reaction as to get optimum coating of nanoparticles on the CNTs and to avoid agglomeration of the CNTs. The temperature generated during the

collapse of a gas-filled cavity is higher in the case of low-vapor pressure solvents.[40] A total of 10% water–DMF solvent resulted in much agglomerated and large ZnO particle size, whereas we observed higher yields for 10% water-EG as a solvent with less agglomeration and small particle size as the vapor pressure of EG (0.06 mm Hg at 20 C) is less than that of DMF (2.7 mm Hg at 20 C). Hence, the temperature at the interfacial region of interest is also higher in the 10% water-EG than in 10% water-DMF solutions. The product is then washed thoroughly with double distilled water and centrifuged using a high speed centrifuging machine at 14,000 rpm, 15°C for about 15 min. The product is washed with double distiller water at least five times and finally washed with ethanol to assist in easy drying of the hybrid nanoparticles. The precipitate was then dried under vacuum at room temperature. The morphology and structure are characterized using XRD and TEM. These hybrid nanoparticles were used for reinforcement in Nylon-6.

Melt Processing and Fabrication of Neat and ZnO/CNTs Infused Nylon-6 Fibers

Different set of extrusions were carried out, with neat Nylon-6, CNTs infused Nylon-6 nanofibers, commercial ZnO nanoparticles infused Nylon-6 fibers and hybrid ZnO/CNTs nanoparticles infused Nylon-6 PNC fibers. The nanoparticles and Nylon-6 powder were carefully measured in the ratio of 1 : 99 by weight. As CNTs have a strong tendency to agglomerate and entangle, they are dry mixed before extrusion.[41,42] The noncontact dry mixing of nanoparticles and Nylon-6 powder were carried out using the centrifugal effect of Thinky machine running at 2000 rpm for about 10 min. The mixing cycle was paused for 5 min after every repetition and then resumed for further mixing. This was done to avoid any temperature rise, which may cause softening of the nylon-6. This process was repeated 7–8 times until deagglomerated mixture of uniform size particles was accomplished.

Nylon-6 and nanoparticles mixtures were further air dried in a dryer for 12 h and extruded using a Wayne Yellow Label Table Top extruder. The extruder has a 19 mm diameter screw, which is driven by a 2HP motor. Thermostatically controlled five heating zones were used to melt the mixture before extrusion, three inside the barrel and two in the die zone at set temperatures of 226°C, 235°C, 243°C, 246°C, and 246°C, respectively. The purpose of these three heaters is to maintain gradually increasing temperature in the molten mass. The process begins when the nanophased dry mixed powder are poured through the feed hopper to get inside the barrel zone of the extruder. As soon as they reach the barrel zone, Nylon-6 starts melting because of high barrel temperature and CNTs are randomly distributed within the liquid matrix. The screw rotation induces the high velocity liquid to experiences enormous shear force. The shear force contributes to the orientation of CNTs. The partially aligned rod shape particles containing liquid Nylon-6 now enters the die zone, which is constructed with a circular plate, 10-cm long steel tubing with 4 mm inner diameter and the die itself. The two heaters at this zone are set at a temperature of 245°C to maintain constant temperature of the flowing mass. One of the heaters is placed after the circular plate and the other one is placed immediately before the die. The circular plate is 15 mm in diameter and contains about 20 orifices, each of which is 2 mm in diameter. As the bulk materials are passing through the plate, they are disintegrated into several branches, and then combined again. This ensures a distributive mixing of the nanoparticles with Nylon-6. Now partially aligned nanoparticles containing liquid Nylon-6 are passed through the 10-cm long steel tube and arrive close to the die. It should be noted that in order to ensure proper alignment of fiber, the size of the die plate and the diameter of the die opening are very critical. Hence, a special type of die was used in this process, which has a converging inlet and narrow outlet (1 mm).This die configuration generates two distinct flow regimes that highly affect the fiber alignments. First, the converging die inlet introduces a converging flow pattern, which in turn aligns the fibers along the streamline direction. Second, the narrow orifice allows the flow pattern to transform into shear flow as it enters the narrow orifice. The shear flow produces additional fiber alignment because of differential shear rate along the boundary layer that orients the fibers in the direction of flow.[43] This is a continuous process and the composite fibers with constant tension were extruded at a screw speed of 10 rpm and feed rate of ~80 g/h. Then the fibers were stabilized by using a set-up of two godet machines and a heater and the fibers were finally wound on a spool using Wayne Desktop Filament Winder at a winding speed of 50 rpm.

Characterization

The X-ray diffraction (XRD) study was carried out with Rigaku D/MAX 2200 X-ray diffractometer to understand the purity, size, and crystalline nature of ZnO coated CNTs nanoparticles. The morphology and size of the ZnO coated CNTs was examined using Transmission electron microscopy (TEM). Samples for TEM examinations were prepared by suspending dried samples in ethanol. A drop of sample suspension was allowed to dry on a copper grid (200 mesh) coated with a carbon film. Once dried, the grid was placed in the TEM. The size and shape of Nylon-6 polymer fibers were estimated using JEOL JSM 5800 SEM. The samples were sputter coated with gold/palladium before carrying out the SEM analysis. Differential scanning calorimetry (DSC) experiments were carried out using a Mettler Toledo DSC 822e from 30°C to 300°C at a heating rate of 5°C/min under nitrogen atmosphere and cooled from 300°C to 30°C at the same rate. Tensile tests for individual fibers were conducted on a Zwick Roell tensile tester equipped with a 20 N Load Cell. The tests were run under displacement control at a crosshead speed of 0.01 1/s strain rate and gage length of 102 mm.

The UV absorption activity for the neat and nano infused Nylon-6 fibers were studied using a Beckman DU.530 UV-vis spectrophotometer. The absorption spectrums for all the fibers were monitored by measuring the UV-vis spectrum in the range of 200–1000 nm. The samples were prepared by dispersing the ~20 mg of finely chopped polymer fibers in 1 mL deionized water.

RESULTS AND DISCUSSION

XRD Characterization

Figure 1 depicts the XRD patterns of: (a) as-received CNTs nanoparticles, (b) as-synthesized ZnO/CNTs nanoparticles with

Applied Polymer SCIENCE

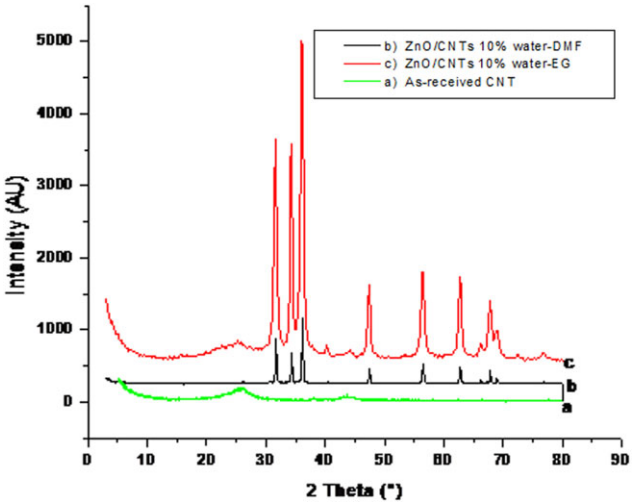

Figure 1. XRD pattern of (a) as-received CNTs nanoparticles (b) ZnO/CNTs-10% water-DMF as solvent (c) ZnO/CNTs-10% water-EG as solvent. [Color figure can be viewed in the online issue, which is available at wileyonlinelibrary.com.]

10% water-DMF as solvent, (c) as-synthesized ZnO/CNTs nanoparticles with 10% water-EG as solvent. The XRD peaks of as-synthesized ZnO/CNTs nanoparticles using both DMF and EG as solvents match very well with the Zincite-syn peaks with the JCPDF # 36-1451 and CNTs with graphite-2H of JCPDF # 41-1487. These results reveal that the as-synthesized ZnO/CNTs nanoparticles are highly crystalline and no impurities were found when compared with the ZnO and CNTs JCPDF files. To estimate the particle sizes from XRD peaks the FWHM (full width half maximum) of the 100% intensity peaks were measured. The increase in the FWHM value (0.562) for the ZnO/CNTs-10% water-EG solvent sample compared with ZnO/CNTs-10% water-DMF (0.232) solvent and the neat CNTs nanoparticles (0.540) clearly indicates that there is a significant reduction in size of the nanoparticles based on the Debye-Scherrer formula and also with TEM analysis.

TEM Characterization

The TEM studies were carried out to understand the extent of ZnO coating on CNTs. Figure 2(a–d) shows the TEM picture of the ZnO/CNTs nanoparticles for both 10% water-DMF and

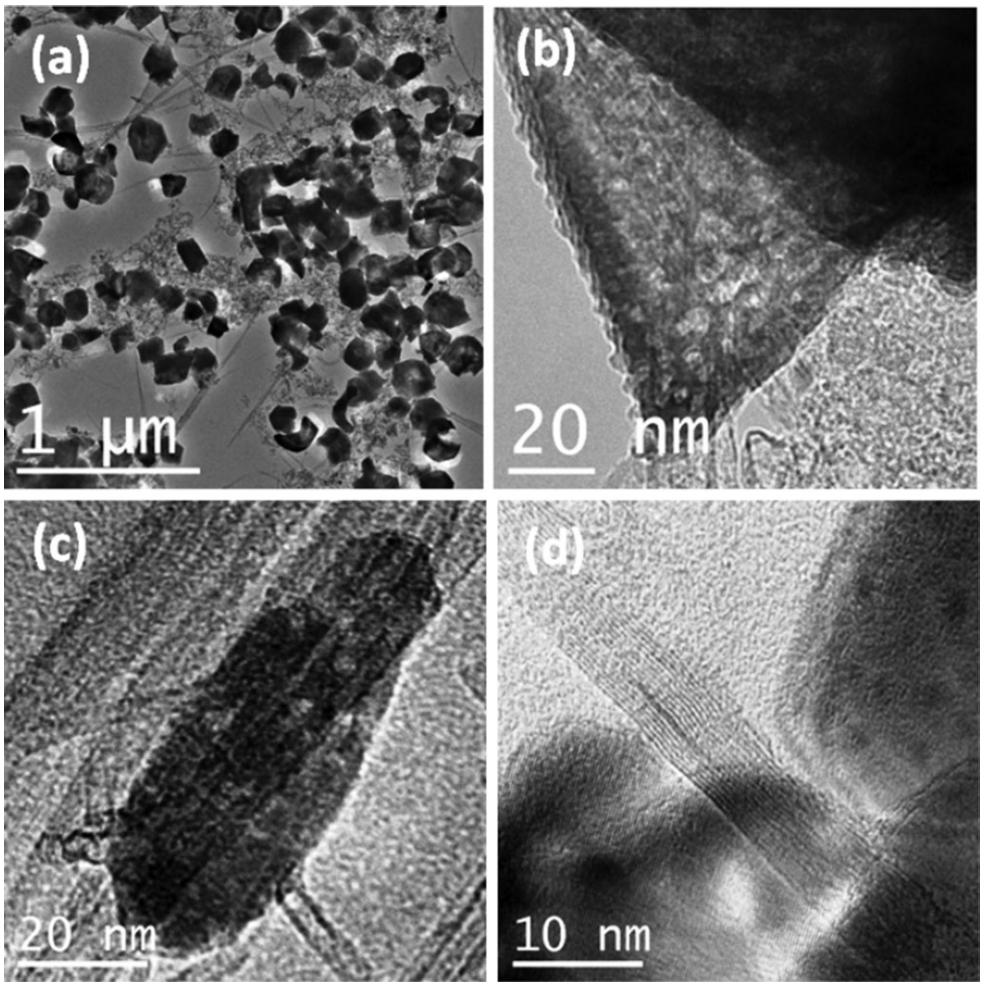

Figure 2. TEM micrograph of ZnO/CNTs nanoparticles with (a) 10% water-DMF, (b) 10% water-DMF at high magnification, (c) 10% water-EG, and (d) 10% water-EG at high magnification.

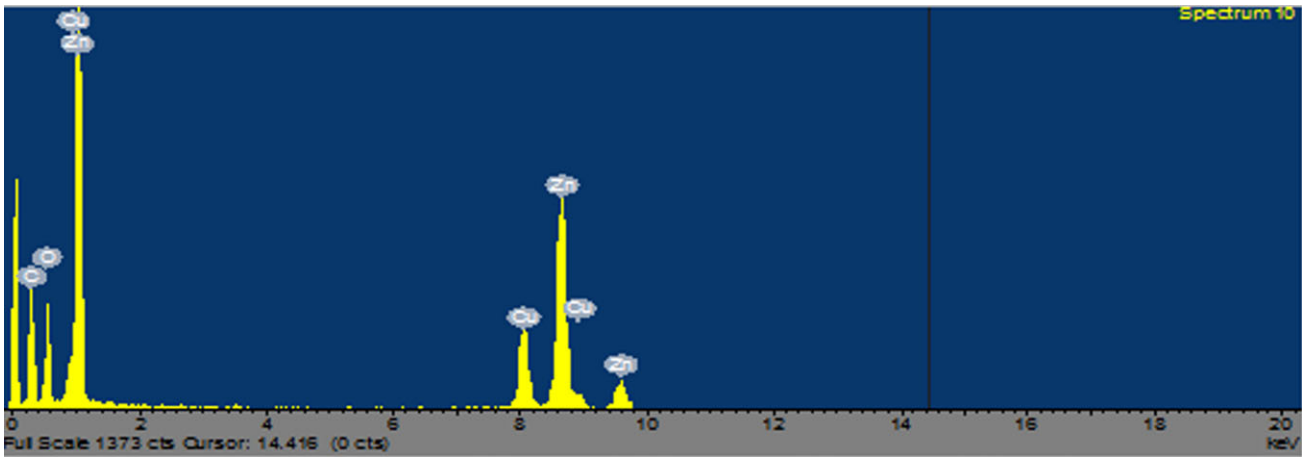

Figure 3. EDS-image of ZnO/CNTs nanoparticles. [Color figure can be viewed in the online issue, which is available at wileyonlinelibrary.com.]

10% water-EG samples respectively. The ZnO/CNTs nanoparticles obtained using water-DMF as solvent is shown in Figure 2 (a and b) at two different magnifications. Figure 2(a) at low magnification shows that the ZnO particles are in large cube shapes and sizes are in the range of 100–200 nm. Figure 2(b) at higher magnification shows that the ZnO particles were surrounding the CNTs. The ZnO/CNTs nanoparticles obtained using water-EG as solvent were shown two different magnifications. At low magnification, Figure 2(c) shows that the particles are in rod shape with ~10 nm in diameter and ~80 nm in length. The TEM micrograph at higher magnification shown in Figure 2(d) represents the lattice structure of the ZnO nanoparticles thus ensuring that the ZnO nanoparticles are highly crystalline in nature. Energy Dispersive Spectroscopic (EDS) analysis were carried out to understand the impurities in as-prepared nanoparticles and shown in Figure 3. These results show that there were no impurities and all the peaks are assigned to ZnO and carbon. The copper peak other than the zinc, oxygen, and carbon correspond to the copper grid, which is used for TEM sample preparation. We have also observed from the TEM analysis that the initial dispersion of CNTs in solvent using in sonochemical reaction is also an important factor to produce uniform coating of ZnO nanoparticles on CNTs surfaces. The better dispersion of CNTs in the initial 10% water-EG solution during the magnetic stirring process results in the uniform distribution, and deagglomeration of CNTs; and hence, the good coating of ZnO nanoparticles on the CNTs surfaces during the ultrasonic irradiation process. It is also well know in the literature the numerous factors influence the acoustic cavitation and sonochemical yields.[44,45] In the bulk solution, factors favoring maximum acoustic cavitation and sonochemical yields are (i) low viscosity, (ii) high surface tension, (iii) low vapor pressure, and (iv) high sound speed. DMF is freely miscible with water, and DMF fulfills all of the aforementioned criteria and ethylene glycol does not. This may be the possible reason for the formation of two different shapes and sizes of ZnO nanoparticles.

SEM Characterization

All of the extruded neat and nano infused Nylon-6 PNC fiber's diameters were measured using SEM analysis. The SEM micrograph shown in Figure 4 is a typical as-extruded fiber diameter. At least 10 samples of each fiber diameters were measured and the average diameter falls in the range of ~80 μ for the sample of ZnO/CNTs Nylon-6 fiber. The size of the fibers was used to carry out the stress strain calculations during the tensile testing characterization of the neat and nanoparticles infused Nylon-6 fibers.

Thermal Response

Differential Scanning Calorimetric (DSC) analyses were used to measure the glass transition temperature (T_g), melting temperature (T_m), and crystallization temperature (T_c) of neat Nylon-6, commercial ZnO infused Nylon-6, CNTs infused Nylon-6, and ZnO/CNTs infused Nylon-6. The data are presented in Table I and shown in Figures 5 and 6. In this study the T_g's were measured as the inflection point of the heat flow curves.[46,47] The Table I clearly shows that the T_g's of extruded Nylon-6 increased from 80–125°C and melting temperatures from 223–225°C with

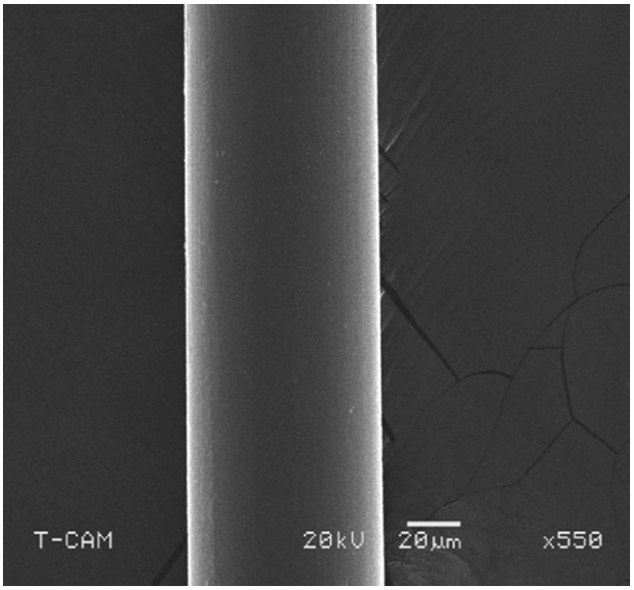

Figure 4. SEM-micrograph of ZnO/CNTs Nylon-6 PNC fiber.

Table I. Thermal Properties of Neat and Nanoparticles Infused Nylon-6 Fibers

Sample	Recrystallization (°C)	Melting Point (°C)	Glass Transition (°C)
Neat Nylon-6	190.7	223.2	79.8
1% CNTs-Nylon-6	195.2	226.2	121.5
1% comr. ZnO-Nylon-6	188.8	223.2	109.1
1% ZnO-CNTs Nylon-6	190.9	225.1	124.6

addition of 1 wt % of ZnO/CNTs. This increase in T_g and melting point is due to the presence of ZnO/CNTs, which may have imposed restriction of molecular mobility at earlier stages. This effect can also be understood in terms of decreasing free volume of polymer. From the concept of free volume, it is known that in the liquid state when free space is high, molecular motion is relatively easy because of the unoccupied volume. As the temperature of the melt is lowered, the free volume would be reduced until there would not be enough free space to allow molecular motion or translation. With the infusion of ZnO/CNTs, this free space is evidently further reduced.[48,49] Melting temperature T_m of polymers that can crystallize such as Nylon has been linked with their chemical structure. Three factors influence this link, chain geometry and regularity, chain stiffness, and hydrogen bonding within Nylon.[50] It has already been demonstrated that nanotubes can act as sites of nucleation for polymer crystals.[51,52] According to Table I, there is no significant difference in the melting temperatures of the neat Nylon 6 and ZnO/CNTs infused Nylon-6. This is confirmed by the close

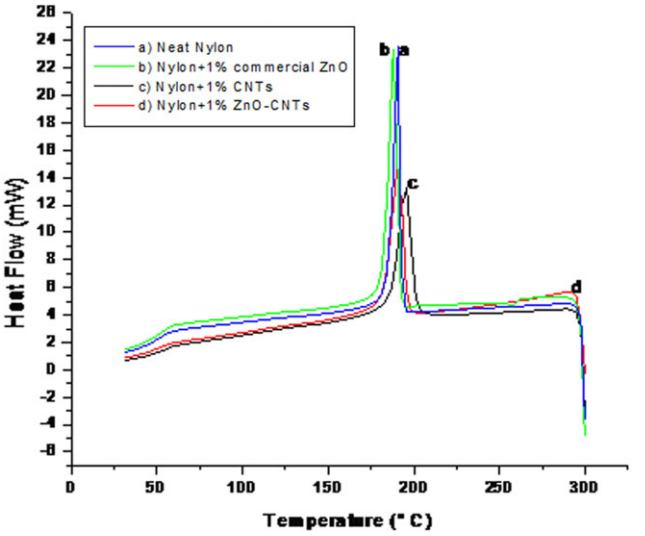

Figure 6. DSC cooling curves of (a) Neat Nylon-6, (b) commercial ZnO-Nylon-6, (c) CNTs-Nylon-6, and (d) ZnO/CNTs-Nylon-6 fibers. [Color figure can be viewed in the online issue, which is available at wileyonlinelibrary.com.]

crystallinity of the neat and nanophased systems. Similar results were observed in our earlier studies as well.[25]

Although changes in the T_m value were not significant; it is interesting to note the effect of ZnO/CNTs on the amorphous region of the DSC thermograms. The amorphous region of a polymer influences elongation properties in such way that if the polymer were highly crystalline we would see lower elongation in mechanical properties. The ZnO/CNTs serve as the tie molecules in the amorphous region of nylon that connect the crystalline regions.[53] In this case, we note the distinct amorphous

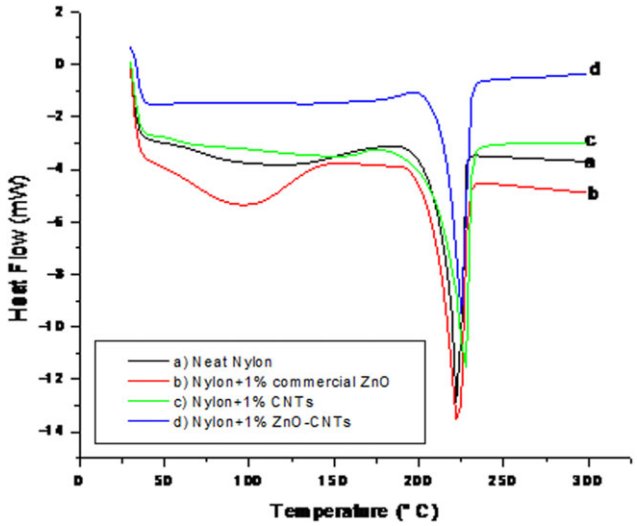

Figure 5. DSC heating curves of (a) Neat Nylon-6, (b) commercial ZnO-Nylon-6, (c) CNTs-Nylon-6, and (d) ZnO/CNTs-Nylon-6 fibers. [Color figure can be viewed in the online issue, which is available at wileyonlinelibrary.com.]

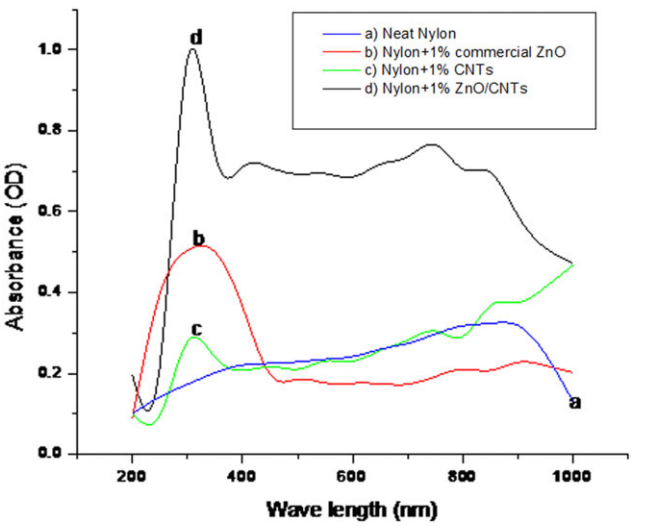

Figure 7. UV/Vis spectral absorption of (a) Neat Nylon-6, (b) commercial ZnO-Nylon-6, (c) CNTs-Nylon-6, and (d) ZnO/CNTs-Nylon-6 fibers. [Color figure can be viewed in the online issue, which is available at wileyonlinelibrary.com.]

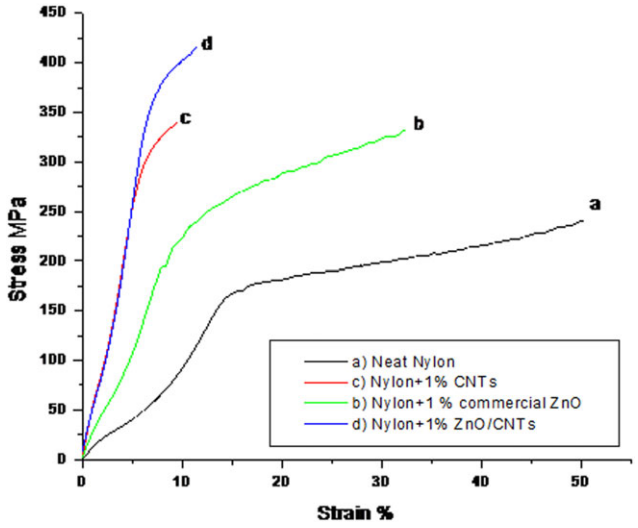

Figure 8. Tensile response of (a) Neat Nylon-6, (b) commercial ZnO-Nylon-6, (c) CNTs-Nylon-6, and (d) ZnO/CNTs-Nylon-6. [Color figure can be viewed in the online issue, which is available at wileyonlinelibrary.com.]

region centered at about 100°C for neat Nylon, shown by DSC plot in Figure 5(a), which correlates with the sample with the highest elongation property such as neat Nylon, shown in Figure 8(d). The near lack of an amorphous region, as found on the thermogram for 1% ZnO/CNTs/Nylon-6 in Figure 8(d), results in the sample with increased mechanical properties and the much lower elongation that are shown in Figure 8(d).

UV Absorption Characterization

The nanoparticles of 1 wt % ZnO/CNTs infused in Nylon-6 fibers along with neat Nylon-6 systems were studied for their UV absorption properties. The UV-absorption spectrums of (a) neat Nylon-6, (b) commercial 1 wt % ZnO-Nylon-6, (c) 1 wt % CNTs-Nylon-6, and (d) 1 wt % ZnO/CNTs Nylon-6 fibers were presented in Figure 7. As expected these results show that the neat Nylon-6 does not show any absorption peaks in the UV range from 200 to 400 nm, whereas the 1 wt % CNTs-Nylon-6 fibers, 1 wt % commercial ZnO-Nylon-6, and 1 wt % ZnO/CNTs–Nylon-6 fibers shows 0.28, 0.5, and 0.98 units, respectively. The absorption peak for 1 wt % CNTs-Nylon-6 is lowest (0.28) compared with the 1 wt % commercial ZnO-Nylon-6 and 1 wt % ZnO/CNTs-Nylon-6 fibers. The hybrid 1% ZnO/CNTs infused Nylon-6 PNC fibers exhibit a strong UV absorption and also a peak shift. The position of plasmon absorption is related to electron density of metal. When decreasing the electron density of metal, the plasmon absorption of metal will be increased.[54] With the coating of ZnO nanoparticles on CNTs, the electron density increases thereby resulting in the reduction of the wide plasmon resonance absorbance as observed in only ZnO/CNTs Nylon-6 nano fibers. The UV absorbance observed for 1 wt % ZnO/CNTs–Nylon-6 fibers is maximum ~1.0 units. These results indicate that PNC fibers can be used for UV absorbing textile applications.

Tensile Properties

To understand the mechanical strength of single fibers of (a) neat Nylon-6, (b) commercial 1 wt % ZnO-Nylon-6, (c) 1wt% CNTs-Nylon-6, and (d) 1 wt % ZnO/CNTs Nylon-6 fibers were tested for their tensile loading and the stress versus strain curves are presented in Figure 8. The experimental results for the ultimate tensile strength and elongation (%) for the neat Nylon-6, 1% CNTs infused Nylon-6, 1% commercial ZnO infused Nylon-6 and 1% hybrid ZnO/CNTs infused Nylon-6 PNC fibers are summarized in Table II. It is shown that the 1% ZnO/CNTs Nylon-6 PNC fibers have the maximum ultimate strength than all the other fibers. The failure stress of the extruded Nylon-6 fibers infused with 1% ZnO/CNTs nanoparticles is about 72.97% higher than the neat extruded Nylon-6 fiber and the improvement in the tensile modulus is 377.38%. This increase of 73% in the tensile strength is very significant and it shows that the ZnO/CNTs nanoparticles have exhibited better interfacial bonding strength. The alignment of the ZnO/CNTs nanoparticles along the direction of extrusion has contributed to better load transfer in the fiber. It can be seen from Figure 8 that 1% CNTs infused Nylon-6 fibers is very hard and brittle and their Young's modulus is the highest, and the 1% commercial ZnO infused Nylon-6 fibers are comparatively very ductile with the 1% CNTs infused Nylon-6 fibers. Whereas the *in situ* synthesized 1% ZnO/CNTs infused Nylon-6 fibers have a very better rigidity and hardness and at the same time they have very high toughness than all the other PNC fibers. Hence, the 1% ZnO/CNTs infused Nylon-6 PNC fibers is superior in strength, rigidity, and toughness of the nanocomposite than compared with the commercial ZnO infused Nylon-6 PNC fibers and as received CNTs infused Nylon-6 PNC fibers. It is believed that the interfacial shear strength between the Nylon-6 and 1% ZnO/CNTs nanoparticles was significantly higher than that was occurred between other systems. The presence of more number of nanoparticles with higher aspect ratios provided increased interfacial interactions, and therefore, high strength and toughness. The Table II summarizes the improvement in the Young's modulus, ultimate strength and the toughness of the 1% ZnO/CNTs infused Nylon-6 PNC fibers compared with other fibers.

Table II. Tensile Properties of Neat and Nanoparticles Infused Nylon-6 Fibers

Type Polymer composite fibers	Tensile Strength, MPa	% Improvement	Tensile Modulus, GPa	Gain/Loss (%) in Modulus
Neat Nylon-6	240	-	0.84	-
1% CNTs-Nylon-6	339	41.3	5.05	501.2
1% ZnO-commercial-Nylon-6	332	38.0	1.91	127.4
1% insitu ZnO/CNTs-Nylon-6	416	73.0	4.01	377.4

CONCLUSIONS

In situ synthesis of hybrid ZnO/CNTs nanoparticles were carried using sonochemical technique. The 10% water-EG solvent reactions successfully yielded pure ZnO nanoparticles of uniform small size and shape coated on the CNTs surfaces. Neat Nylon-6, commercial ZnO infused, pristine CNTs infused and hybrid ZnO/CNTs infused Nylon-6 polymer composites were fabricated using single screw melt extruder. XRD, TEM studies reveal that ZnO nanoparticles were uniformly coated on CNTs surfaces. The improvement in ultimate tensile strength and elastic modulus is attributed to the alignment of the ZnO/CNTs nanoparticles along the direction of extrusion. The increase in thermal stability and crystallinity of ZnO/CNTs infused Nylon-6 PNC is correlated with the better cross linking between the nanoparticles and the polymer matrix. The *in situ* 1% ZnO/CNTs Nylon-6 PNC fibers demonstrated to have better UV absorption activity than the commercially available ZnO nanoparticles infused Nylon-6 PNC fibers. These initial results suggest that the PNC fiber fabricated in this project can be used for UV-absorbing textile application.

ACKNOWLEDGMENTS

The authors like to thank the National Science Foundation for their financial support through NSF-RISE# 1137682.

REFERENCES

1. Yon J.-N.; Jamie R. L. *Sci. Total Environ.* **2008**, *400*, 396.
2. Huang, M. H.; Mao, S.; Feick, H.; Yan, H. Q.; Wu, Y. Y.; Kind, H.; Weber, E.; Russo, R.; Yang, P. D. *Science* **2001**, *292*, 1897.
3. Wang, Z. L. *J. Phys. Condens. Matt.* **2004**, *16*, 829.
4. Yang, K.; Ozisik, R. *Polymer* **2006**, *47*, 2849.
5. Jiang, Z. Y.; Xie, Z. X.; Zhang, X. H.; Lin, S .C.; Xu, T.; Xie, S. Y.; Huang, R. B.; Zheng, L. S. *Adv. Mater.* **2004**, *16*, 904.
6. Zhua, L. P.; Liao, G. H.; Huangc, W. Y.; Mac, L. L.; Yang, Y.; Yuc, Y.; Fu, S. Y. *Mater. Sci. Eng. B* **2009**, *163*, 194.
7. Starowicz, M.; Stypula, B. *Eur. J. Inorg. Chem.* **2008**, *869*, 72.
8. Singh, S.; Thiyagarajan, P.; Kant, K. M.; Anita, D.; Thirupathiah, S.; Rama, N. *J. Phys. D Appl. Phys.* **2007**, *40*, 6312.
9. Oaki, Y.; Imai, H. *Langmuir* **2005**, *21*, 863.
10. Huang, Z.; Zheng, X.; Yan, D.; Yin, G.; Liao, X.; Kang, Y. *Langmuir* **2008**, *24*, 4140.
11. Zhou, J.; Xu, N. S.; Wang, Z. L. *Adv. Mater.* **2006**, *18*, 2432.
12. Adams, L. K.; Lyon, D. Y.; Alvares, P. J. J. *Water. Res.* **2006**, *40*, 3527.
13. Zhang, X.; Sun, H.; Zhang, Z.; Niu, Q.; Chen, Y.; Crittenden, J. C. *Chemosphere* **2007**, *67*, 160.
14. Singh, S. C.; Gopal, R. *Phys. E* **2008**, *40*, 724.
15. He, Y.; Sang, W.; Wang, J.; Wu, R.; Min, J. *Mater. Chem. Phys.* **2005**, *94*, 29.
16. He, Y.; Sang, W.; Wang, J.; Wu, R.; Min, J. *J. Nanoparticles Res.* **2005**, *7*, 307.
17. Iijima, S. *Nature* **1991**, *354*, 56.
18. Wong, E. W.; Sheehan, P. E.; Lieber, C. M. *Science* **1997**, *277*, 1971.
19. Wang, C.; Guob, Z. X.; Fu, S.; Wu, W.; Zhu, D. *Prog. Polym. Sci.* **2004**, *29*, 1079.
20. Dalton, A. B.; Collins, S.; Munoz, E.; Razal, J. M.; Ebron, V. H. Ferraris, J. P. *Nature* **2003**, *423*, 703.
21. Gong, X. Y.; Liu, J.; Baskaran, S.; Voise, R. D. Young, J. S. *Chem. Mater.* **2000**, *12*, 1049.
22. Jin, Z. X.; Pramoda, K. P.; Goh, S. H. Xu, G. Q. *Mater. Res. Bull.* **2002**, *37*, 271.
23. Qian, D.; Dickey, E. C.; Andrewsm R.; Rantell, T. *Appl. Phys. Lett* **2000**, *76*, 2868.
24. Cadek, M.; Coleman, J. N.; Barron, V.; Hedicke, K.; Blau, W. *J Appl. Phys. Lett.* **2002**, *81*, 5123.
25. Rangari, V. K.; Yousuf, M.; Jeelani, S.; Pulikkathara M. X.; Khabashesku, V. N. *Nanotechnology* **2008**, *19*, 245703.
26. Kim, H.; Sigmund, W. *Appl. Phys. Lett* **2002**, *81*, 2085.
27. Sun, J.; Gao, L.; Iwasa, M. *Chem. Commun.* **2004**, 832.
28. Jiang, L.; Gao, L. *Mater. Chem. Phys.* **2005**, *91*, 313.
29. Chen, C. S.; Chen, X. H.; Yi, B.; Liu, T. G.; Li, W. H.; Xu, L. S.; Yang, Z.; Zhang, H.; Wang, Y. G. *Acta Mater.* **2006**, *54*, 5401.
30. Bae, S. Y.; Seo, H. W.; Choi, H. C.; Park, J. *J. Phys. Chem. B* **2004**, *108*, 12318.
31. Chrissanthopoulos, A.; Baskoutas, S.; Bouropoulos, N.; Dracopoulos, V.; Tasis, D.; Yannopoulos, S. N. *Thin Solid Films* **2007**, *515*, 8524.
32. Rangari, V. K.; Diamant, Y.; Gedanken, A. *Chem. Mater.* **2000**, *12*, 2301.
33. Becheri, A.; Durr, M.; Nostro, P. L.; Baglioni, P. *J. Nanopart. Res.* **2008**, *10*, 679.
34. Yang, K.; Ozisik, R. *Polymer* **2006**, *47*, 2849.
35. Stephen, M.; David, G. *K. B. Polymer* **2005**, *46*, 11424.
36. Akhtar, S. K.; Farrokh, B. *Int. J. Plast* **2006**, *22*, 1506.
37. Rangari, V. K.; Mohammad, Y. S.; Mahfuz, H.; Jeelani, S. *Mater. Sci. Eng. A* **2009**, *500*, 92.
38. Wang, S. F.; Gu, F.; Lu, M. K.; Zhoua, G. J.; Zhang, A. Y. *J. Cryst. Growth* **2006**, *289*, 621.
39. Pol, V. G. Srivastava, D. N.; Palchik, O.; Palchik, V.; Slifkin, M. A.; Weis, A. M.; Gedanken, A. *Langmuir* **2002**, *18*, 3352.
40. Suslick, K. S.; Hammerton, D. A. *IEEE Trans. Sonics Ultrason.* **1986**, SU–33, 143.
41. Mahfuz, H.; Adnan, A.; Rangari, V. K.; Jeelani, S. *Int. J. Nanosci.* **2005**, *4*,55.
42. Li, Y.; Guo, Z.; Yu, J. *Macromol. Mater. Eng.* **2005**, *290*, 649.
43. Tanoue, S.; Hasook, A.; Itoh, T.; Yanou, M.; Iemoto, Y.; Unryu, T. J. *Appl. Polym. Sci.* **2006**, *101*, 1165.
44. Flynn, H. G. In Physical Acoustics: Principles and Methods; Mason, W. P., Ed.; Academic Press: New York, **1964**; p 165.

45. Rangari, V. K.; Diamant, Y.; Gedanken, A. *Chem. Mater.* **2000**, *12*, 2301.

46. Antonio G. L.; Fabien, C.; Michel, D.; Jean P. P. *Macromolecules* **2002**, *35*, 6291.

47. Rangari, V. K.; Yuri, K.; Cohen, S.; Aurbach, D.; Palchik, O.; Felner, I.; Gedanken A. *J. Mater. Chem.* **2000**, *10*, 1125.

48. Chen, K.; Vyazovkin, S. *Macromol. Chem. Phys.* **2006**, *207*, 587.

49. Liu, T. X.; Tong, Y. J.; Zhang, W. D. *Compos. Sci. Technol.* **2007**, *67*, 406.

50. Aharoni, S. n-Nylons: Their Synthesis, Structure, and Properties; John Wiley and Sons, Ltd.: West Sussex, UK, **1998**; p 252–253.

51. Li, L.; Li, C. Y.; Ni, C. *J. Am. Chem. Soc.* **2006**, *128*, 1692.

52. Zhang, S.; Minus, M.; Zhu, L.; Wong, C.P.; Kumar, S. *Polymer* **2008**, *49*, 1356.

53. Courtney, T. Mechanical Behavior of Materials; McGraw Hill: New York, USA, **2000**; p 175–292.

54. Shan, G.; Zhong, M.; Wang, S.; Li, Y.; Liu, Y. *J. Colloid. Int. Sci.* **2008**, *326*, 392.